Two-Dimensional Hα Emission Measurements Using the Multi-Channel Hα Array System in GAMMA 10/PDX

Tomoya YAMASAKI, Masayuki YOSHIKAWA, Junko KOHAGURA, Yoriko SHIMA, Hiroyuki NAKANISHI, Shun SUTO, Tomoya MOURI, Mizuki SAKAMOTO and Yousuke NAKASHIMA

Plasma Research Center, University of Tsukuba, 1-1-1 Tennodai, Tsukuba, Ibaraki 305-8577, Japan

(Received 15 April 2019 / Accepted 7 April 2020)

We developed a multi-channel Hα array system to measure two-dimensional (2D) radial profiles of Hα emissivity in the central cell of the tandem mirror GAMMA 10/PDX. It consists of a 2D optical collection system, which contains twelve channels of lenses, Hα filters, and bundled optical fibers in vertical and horizontal directions. To study Hα emission behavior and its fluctuation in the hot-ion mode plasma experiments with additional plasma heating application, we used the modified Phillips-Tikhonov tomography method. After applying the fast Fourier transform analysis to the 2D Hα emissivity profiles, we could successfully obtain the 2D fluctuation images for the first time. These results are useful for the detailed study of fluctuations in magnetically confined plasma.

Keywords: Hα measurement, Phillips-Tikhonov method, tomography, tandem mirror GAMMA 10/PDX

DOI: 10.1585/pfr.15.1401035

1. Introduction

Spectroscopic measurements are critical for fusion plasma experiments and contain essential information about fusion plasma, such as plasma particle confinements, impurity transport, plasma density, and plasma temperature [1–4]. In GAMMA 10/PDX, there are some spectroscopic measurement systems, such as a visible and ultraviolet spectroscopic system, which can measure the radial profiles of plasma radiation, multi-wavelength measurement spectrometers, as well as the filter type Hα line emission measurement systems. The multi-channel Hα array system is used to study plasma behavior and plasma fluctuation. GAMMA 10/PDX is an effectively axisymmetric minimum-B anchored tandem mirror with a thermal barrier at both end-mirrors (Fig. 1) [3–5]. The x-axis and y-axis are perpendicular to the magnetic field in the vertical and horizontal directions, respectively. In addition, the z-axis is parallel to the magnetic field. The plasma is created using plasma guns and heated and sustained using ion cyclotron heating (ICH) systems. In addition to ICH, the electron cyclotron heating (ECH) can be applied to produce the electron and ion confinement potential in the plug and barrier cells.

The multi-channel Hα array system is then installed in the central cell of GAMMA 10/PDX (Fig. 1). The reconstruction method is essential to obtain the spatial distribution of Hα emissivity from the line-integrated intensity of radiation. Moreover, the neutral particle density from the reconstructed emissivity image after use of the optical

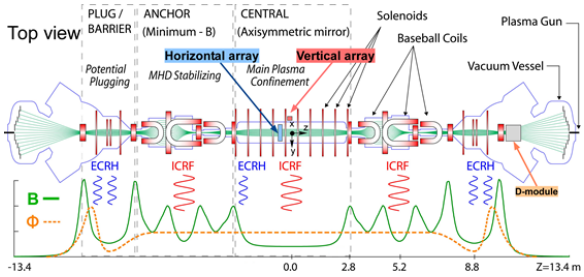

Fig. 1 Schematic view of GAMMA 10/PDX indicating the position of the vertical (red) and horizontal (blue) Hα array systems.

radiation model of the collisional-radiative model can be derived [2, 4, 6–9]. By applying this reconstruction data to the fast Fourier transform (FFT) analysis, it is possible to observe the temporal evolution of the emissivity fluctuation of radiation.

We constructed the analysis method for the two-dimensional (2D) Hα line emission measurement system to obtain the 2D Hα emissivity image and the FFT-analyzed image of Hα emissivity fluctuations in GAMMA 10/PDX for the first time.

2. Hα Array System in GAMMA 10/PDX

Figure 2 displays the side view of the 2D Hα line emission measurement system. The vertical and horizontal array systems for the 2D optical correction system were

author's e-mail: yosikawa@prc.tsukuba.ac.jp

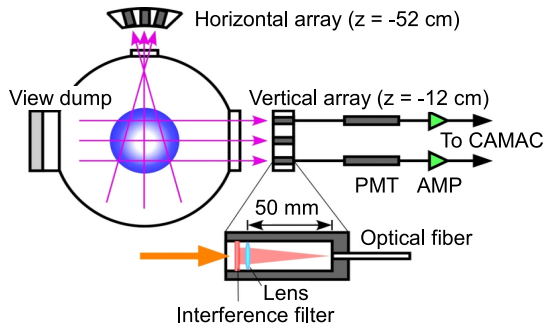

Fig. 2 Side view of the two-dimensional Hα line emission measurement system in the GAMMA 10/PDX central cell.

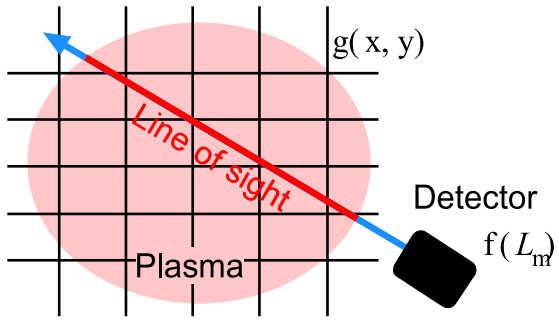

Fig. 3 Image of mesh and the line of sight.

installed at z = −12 and −52 cm, respectively. Each optical collection system consists of twelve collection lenses (f = 30 mm and ϕ = 20 mm), Hα filters (λ = 656.3 nm and $\lambda_{1/2}$ = 3.3 nm), bundled optical fibers (7,104 mm, ϕ = 3.8 mm), the photomultiplier tubes (Hamamatsu Photonics, R1547), and the preamplifiers in vertical and horizontal directions. The outputs of the preamplifiers led to the data recording the CAMAC system. The absolute calibration of the wavelength sensitivity of the system was carried out using a tungsten filament lamp. The spatial resolution and the time resolution of the system were 2 cm and 0.02 ms, respectively.

3. Tomography Method

Tomography is a non-invasive imaging tool to observe the inner structure of plasma. This is an analytical method that reconstructs the spatial distribution of a 2D cross-section by solving the inverse problem. There are various analytical methods, and so far the algebraic reconstruction technique has been previously used in GAMMA 10/PDX [3]. The advantage of this method is that it performs simple calculation with a short calculation time. However, in reconstructing the hollow plasma radial distribution, an appropriate initial value is required. Furthermore, the resulting reconstructed image is not smooth. Therefore, we investigated the construction of a tomography analysis method that does not require an initial value and results in smooth distribution. The tomography in the plasma research field requires a short calculation time. In GAMMA 10/PDX, we adopted a series expansion method (model fitting) in soft X-ray tomography [10]. This is an analytical method that numerically performs the reciprocal of the product and reconstructs the spatial distribution of the 2D cross-section. This method is restricted by the series model, meaning that if the number of measurement points is low, the resolution tends to be poor. Thus, a tomography analysis method, that is strong against gaze loss and can obtain a high resolution, is required. Various spatial distributions can be considered for Hα ray measurement. For example, it must be applied to various shapes. In consideration of these conditions, we are utilizing the Phillips-Thikhonov (PT) method, a recently developed calculation code using the technique.

3.1 Phillips-Thikhonov method

The PT calculation method is shown below. Assuming that the cross-section to be reconstructed is mesh, as shown in Fig. 3, the line integral f (L_m) appears as follows:

$$\begin{aligned} &\mathrm{f}(L_m) = \int_{L_m} \mathrm{g}(\mathrm{x},\mathrm{y})\mathrm{d}l \\ \Rightarrow\ &\mathrm{f} = \mathrm{W}\cdot\mathrm{g} \\ &\mathrm{f} = \mathrm{W}_{\mathrm{m},1}\mathrm{g}_1 + \mathrm{W}_{\mathrm{m},2}\mathrm{g}_2 + \ldots + \mathrm{W}_{\mathrm{m,n}}\mathrm{g}_\mathrm{n}, \end{aligned} \tag{1}$$

where g(x, y) reflects the local amount of emissivity before reconstruction, W and f represent the geometrical system matrix and the measured value, respectively, and L_m indicates the length of the line of sight.

The local quantity g(x, y) is derived from the known W and measured value of f. The mean square error of Eq. (1) is expressed by the following equation:

$$\mathrm{J} = \|\mathrm{f} - \mathrm{W}\cdot\mathrm{g}\|^2/\mathrm{M}. \tag{2}$$

Minimizing J can be indicated by the mean square error plus the signal variation,

$$\left\|\mathrm{f} - \mathrm{W}\cdot\mathrm{g}\right\|^2/\mathrm{M} + \gamma\left|\mathrm{L}\cdot\mathrm{g}\right|^2 \rightarrow \min. \tag{3}$$

This results in a minimization problem with positive undetermined multiplier γ as a parameter. The partially differentiating Eq. (3) and solving for g(γ) with the solution as zero yields the following equation:

$$\begin{aligned} &\frac{\partial \mathbf{J}}{\partial \mathbf{g_i}} = 0, \\ &\mathrm{g}(\gamma) = (\mathrm{W}^\mathrm{T}\cdot\mathrm{W} + \mathrm{M}\gamma\mathrm{L}^\mathrm{T}\cdot\mathrm{L})^{-1}\cdot\mathrm{W}^\mathrm{T}\cdot\mathrm{f}, \end{aligned} \tag{4}$$

$$\mathrm{L} = \frac{1}{2}\begin{pmatrix} -4 & 1 & 0 & \cdots & 0 & 1 & 0 & \cdots & \cdots & \cdots & 0 \\ 1 & -4 & 1 & 0 & \cdots & 0 & 1 & 0 & \cdots & \cdots & 0 \\ 0 & 1 & -4 & 1 & 0 & \cdots & 0 & 1 & 0 & \cdots & 0 \\ \cdots & \cdots & \cdots & \cdots & \cdots & \cdots & \cdots & \cdots & \cdots & \cdots & \cdots \\ 0 & \cdots & \cdots & 0 & 1 & 0 & \cdots & 0 & 1 & -4 & 1 \\ 0 & \cdots & \cdots & \cdots & 0 & 1 & 0 & \cdots & 0 & 1 & -4 \end{pmatrix}, \tag{5}$$

where g(γ) is the reconstructed image, γ is the optimal regularization parameter, L is a Laplacian matrix, and M is the number of data. As the solution g(γ) is a function dependent on γ, we introduced a Generalized Cross Validation minimization criterion to optimize γ [11].

4. Experimental Results

A plasma was produced by the application of ICH from t = 50 - 240 ms and for additional heating with the application of B-ECH from 130 - 170 ms and P-ECH from 150 - 170 ms. Figure 4 demonstrates the time evolutions of diamagnetism (red line) and the electron line density (blue line). The electron line density is observed by the microwave interferometer at z = −60 cm. When applying B-ECH, the diamagnetism increased, and the electron line density remained constant. In contrast, with additional application of P-ECH, the electron line density at the center position increased and the diamagnetism decreased.

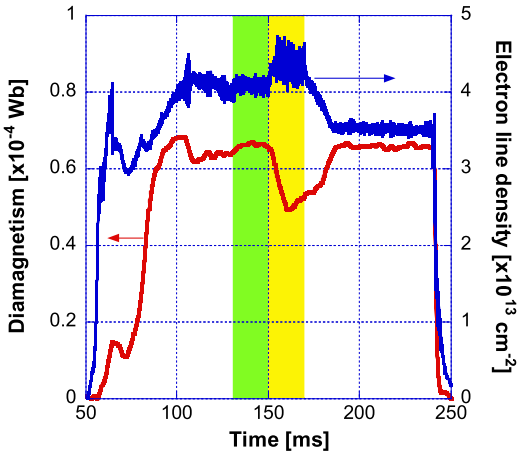

Fig. 4 Time-dependent electron line density (blue line) and diamagnetism (red line) with B-ECH (green hatched region) and P/B-ECH (yellow hatched region).

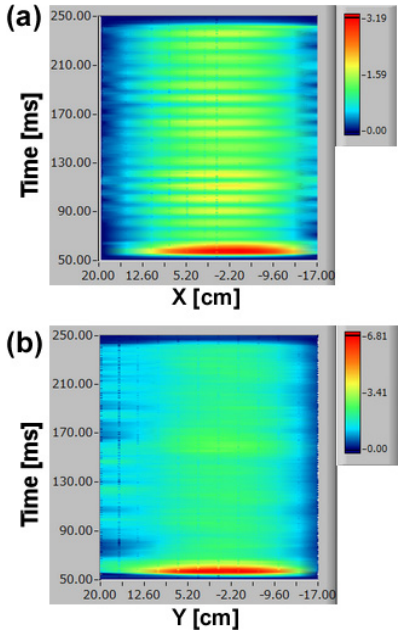

Fig. 5 Time-dependent Hα line emissions of the vertical array (a) and horizontal array (b).

Figure 5 shows the time evolution of the radial distribution of Hα radiation. The vertical direction and horizontal direction of Hα radiations are indicated in (a) and (b), respectively. The x-axis, y-axis, and z-axis indicate the position in cm, time in ms, and radiation intensity in μW/str/nm/mm^2, respectively. Figure 6 reflects the tomography reconstructed Hα emissivity cross-sections using the PT method at t = 151 ms. The maximum emission region is shifted approximately 2 cm in the positive x-direction from the plasma center. We calculated 2D images of Hα emissivity of the plasma duration using the PT method. Figure 7 indicates the time evolutions of the FFT-analyzed electron line density (a) and Hα radiation inten-

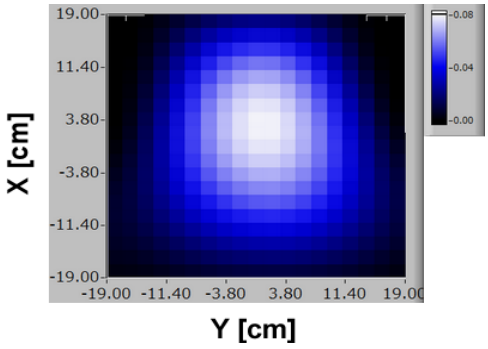

Fig. 6 Reconstructed two-dimensional Hα emissivity.

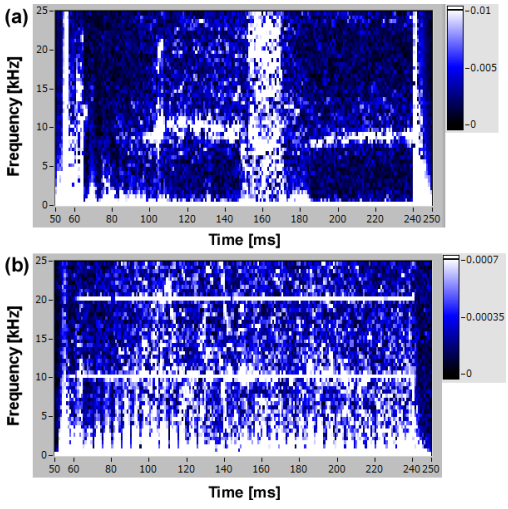

Fig. 7 Fast Fourier transform (FFT) analysis of electron line density (a) and Hα radiation (b).

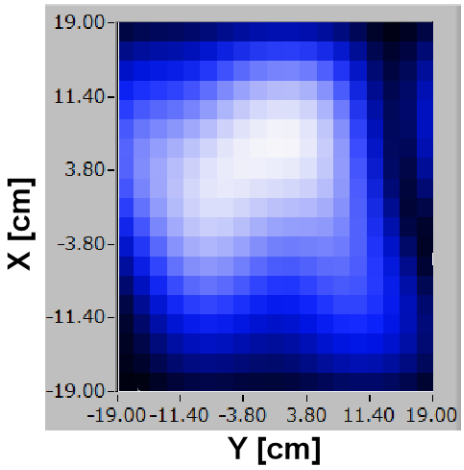

Fig. 8 Two-dimensional Hα fluctuation intensity obtained after the fast Fourier transform (FFT) analysis of the tomography image of emissivity at a frequency of 11 kHz at t = 151 ms.

sity (b) fluctuations at the plasma center. A strong fluctuation was observed at the frequency range of 7 - 12 kHz on the electron line density fluctuation. In the results of the Hα radiation intensity FFT analysis, something similar to noise was strongly observed at the frequencies of 10 and 20 kHz. This was thought to be a noise originating from the ICH system. The fluctuation obtained in the Hα radiation intensity originated from the electron density fluctuation. Figure 8 indicates the 2D distribution of the fluctuation intensity at a frequency of 11 kHz after the calculation of the FFT analysis of each pixel of 2D Hα emissivity images from t = 150.5 ms to 151.5 ms. Fluctuations were observed in the entire space, and it was thought that the stronger fluctuation regions were observed in the upper region of the plasma.

5. Summary

We developed a new tomography method of the PT method for a 2D Hα line emission measurement system of the tandem mirror GAMMA 10/PDX and applied it to the hot-ion mode plasma experiment to obtain the 2D Hα emission image and FFT-analyzed 2D Hα emissivity fluctuation image. We successfully obtained the reconstructed 2D Hα emissivity images. By performing an FFT analysis on the obtained time-dependent 2D reconstructed Hα emissivity images, we could obtain the time evolution of 2D Hα fluctuation distribution. Finally, we may now study the plasma fluctuation in more detail using this 2D fluctuation distribution analysis method.

Acknowledgments

The authors would like to thank members of the GAMMA 10 group of the University of Tsukuba for their collaboration. This work was partly supported by the Ministry of Education, Culture, Sports, Science and Technology, Grant-in-Aid for Scientific Research in Priority Areas, No 16082203 and NIFS collaboration research program, No NIFS04KUGM009.

[1] H.R. Griem, *Principles of Plasma Spectroscopy* (Cambridge University Press, Cambrige, 1997).
[2] M. Goto *et al.*, Phys. Plasmas **10**, 1402 (2003).
[3] M. Yoshikawa *et al.*, Trans. Fusion Technol. **35**, 273 (1999).
[4] M. Yoshikawa *et al.*, J. Plasma Fusion Res. SERIES **6**, 685 (2004).
[5] Y. Nakashima *et al.*, Nucl. Fusion **57**, 116033 (2017).
[6] T. Fujimoto, Nucl. Fusion **28**, 1255 (1988).
[7] S. Sasaki *et al.*, Fusion Eng. Des. **34-35**, 747 (1997).
[8] K. Sawada and T. Fujimoro, Phys. Rev. E **49**, 5565 (1994).
[9] T. Kato *et al.*, Fusion Eng. Des. **34-35**, 25 (1997).
[10] M. Hirata, Nucl. Instrum. Methods **A 477**, 210 (2002).
[11] G.H. Golub, M. Heath and G. Wahba, Technometrics **21**, 215 (1979).